Novel photosensitive glasses

H. Ebendorff-Heidepriem, C. Riziotis, E. R. Taylor
Optoelectronics Research Centre, University of Southampton, SO17 1BJ, U.K.

Fluoride phosphate and ultraphosphate glasses doped with europium, cerium, terbium and lead ions were melted under oxidizing and reducing conditions. Their photosensitivity was examined by UV laser-induced absorption and waveguide writing. Strong waveguides are created for Eu^{2+}, Ce^{3+} and Tb^{3+} dopants. High long-term and thermal stability of laser-induced absorption is observed for Eu^{2+} doped glass. The waveguide creation is explained by the color center model.

1. Introduction

Fundamental devices in the field of optoelectronics and photonics are glass fibers and waveguides with diverse functions and properties. In the last decade, photosensitivity of glasses has received much attraction. A high photosensitivity enables the imprinting of special structures into glasses by lasers as a result of refractive index changes. This phenomenon is used to write directly gratings and waveguides into glasses, which has an enormous impact on the manufacturing, tailoring and efficiency of optical devices.

Photosensitivity of glasses is well known and has been widely studied in germanium-doped silica fibers[1]. Recently, photosensitivity of other optical glasses and especially the search for dopants increasing the photosensitivity is of great practical importance[2,3]. Fluoride phosphate and phosphate glasses are attractive materials for photonic devices[4,5]. Their photosensitivity has been only slightly studied. They received attention due to their athermal properties. The impact of several dopants and glass melting conditions on the photosensitivity is of special interest.

In this paper, two different base glasses, fluoride phosphate (FP) and ultraphosphate (UP), doped with europium, cerium, terbium and lead ions were melted under oxidizing and reducing conditions. The photosensitivity is examined by direct illumination and waveguide writing using UV lasers. Waveguide writing efficiency is compared with laser-induced optical absorption. Furthermore, dynamics and thermal behaviour of photosensitivity is studied using different laser powers (cw, pulsed), exposure times and isochronal annealing.

2. Experimental

Batch compositions of the base glasses and dopant concentrations are reported in Tables 1 and 2. The dopant concentrations were calculated from the amount of dopant oxide or fluoride added to the base glass batch. For the Eu^{2+} doped samples, the summary of both Eu^{2+} and Eu^{3+} ions is known by this calculation. Using fluorescence spectroscopy, the amount of Eu^{2+} ions in the $FP_M/Eu^{2+}/0.3$ sample could be estimated to be about 30% of the whole dopant concentration. The Eu^{2+} concentrations of the other samples are determined from the Eu^{2+} peak absorption intensity at 245 nm relative to the one of the $FP_M/Eu^{2+}/0.3$ sample.

For glass synthesis, raw materials of high purity suitable for optical glasses were used. The glasses melted under oxidizing conditions were prepared by conventional melting procedure of raw material batches at elevated temperatures using platinum crucibles for the FP glasses and silica crucibles for the UP glasses in ambient or oxygen atmosphere. The glass melts were poured into graphite moulds and then slowly annealed to room temperature. The Eu^{2+} doped samples were prepared under reducing melting conditions by remelting the starting Eu^{3+} doped glasses in carbon crucibles in argon atmosphere. The glass melts cooled in the crucibles to room temperature. After annealing the glasses were cut and polished into samples for optical absorption measurements and laser exposure experiments.

Table 1: Batch compositions of the base glasses studied

Base glass	Batch composition (mol%)
FP_M	10 $Sr(PO_3)_2$ – 56 $(Mg,Ca,Sr)F_2$ – 34 AlF_3
FP_{Cl}	10 $Sr(PO_3)_2$ – 46 $(Mg,Ca,Sr)F_2$ – 34 AlF_3 – 10 $SrCl_2$
FP	9 P_2O_5 – 60 $(Mg,Ca,Sr)F_2$ – 31 AlF_3
UP	65 P_2O_5 – 31 $(Mg,Ca,Ba,Zn)O$ – 4 Al_2O_3

Table 2: Dopant concentration and effective thickness at laser wavelengths of the glasses

Glass designation	Dopant concentration* (10^{19} ions cm^{-3})	Melting conditions	Effective thickness (mm)	
			@ 244 nm	@ 248 nm
$FP_{(M)}$ / undoped / ox	-	oxidizing	>10	>10
$FP_{(M)}$ / undoped / red	-	reducing	>10	>10
FP_M / Eu^{2+} / 0.3	0.3	reducing	0.52	0.53
FP / Eu^{2+} / 0.2	0.2	reducing	0.81	0.81
FP_{Cl} / Eu^{2+} / 0.3	0.3	reducing	0.47	0.47
FP_{Cl} / Eu^{2+} / 0.2	0.2	reducing	0.84	0.87
FP / Ce^{3+} / 1.0	1.0	oxidizing	0.60	0.58
FP / Ce^{3+} / 0.5	0.5	oxidizing	1.1	1.1
FP / Pb^{2+} / 1.0	1.0	oxidizing	4.4	6.8
UP / undoped	-	oxidizing	5.1	5.4
UP / Tb^{3+} / 1.0	1.0	oxidizing	4.9	5.0

* for Eu^{2+}: absolute error ±30%, relative error ±10% (see text)
for Ce^{3+}, Pb^{2+}, Tb^{3+}: absolute error ±10%

Absorption spectra were recorded at room temperature using a double-beam spectrophotometer. The measured absorbance spectra, $E(\lambda)$, are defined as E = log(100/transmission%). The spectra shown are corrected for reflection and scattering by subtraction of a constant baseline value, E_0 , at wavelengths where sample absorption is negligible.

Laser exposure experiments were employed using cw frequency-doubled argon ion laser operating at 244 nm (50-150 mW, ca. 3-10 μm spot diameter, 10-500 mm/min scan speed) or pulsed KrF excimer laser operating at 248 nm (300 mJ/cm^2/pulse, 5 Hz repetition rate, ca. 20 ns pulse length). In the case of the KrF laser, a sample area of 5mm diameter was fully exposed by the laser beam. In the case of the argon ion laser, the laser beam was focused to several μm incident on the glass surface. The samples were positioned on a vacuum chuck connected to a computer controlled translation stage, which shifted perpendicularly to the incident UV laser beam at different speeds as illustrated in Figure 1. The guiding structures were characterized by launching light of a fiber-coupled HeNe laser at 633 nm. In order to check the possible presence of laser-induced surface effects such as relief or ablation related phenomena, the samples were observed with an optical microscope and surface profilometer runs were performed.

3. Results and Discussion

The absorption spectra of the samples before laser exposure are shown in Figure 2. The intense UV absorption bands of Eu^{2+}, Ce^{3+} and Tb^{3+} ions are due to allowed 4f-5d transitions[6]. The shift of the UV edge in the Pb^{2+} doped sample results from intense 6s-6p absorption of Pb^{2+} ions[7]. For characterization of transmission and absorption at the laser wavelengths, the effective penetration depth of the laser beam, d_{eff}, has been calculated from absorption spectra by $d_{eff} = d_{sample}/[2.303\times(E-E_0)]$, where d_{sample} is the thickness of the samples used for recording the absorption spectra. High Eu^{2+} and Ce^{3+} concentrations result in small effective thickness of about 0.5 mm. By contrast, the effective thickness of the Pb^{2+} and Tb^{3+} doped glasses is larger than the thickness of the samples used for the laser exposure experiments.

The disappearance of the characteristic Eu^{2+} absorption at 245 nm already after 100 pulses laser irradiation (Figure 3) indicates very fast and complete photooxidation of Eu^{2+}. The UV absorption simultaneously induced is caused by intrinsic electron defect centers, which are formed in conjunction with photooxidation[8]. The destruction of the intense Eu^{2+} absorption causes pronounced bleaching at the laser wavelength of 248 nm. The laser-induced absorption increases with increasing Eu^{2+} concentration before illumination (Figure 4). In addition, it is very stable at room temperature as well as elevated temperatures. No significant recovery was observed more than 3 years after exposure (Figure 3) and after isochronal annealing at 100 °C and 200 °C for 1 hour (Figure 4). The change in the absorption spectrum after annealing at 400 °C for 1 hour (Figure 4) resembles the difference in the spectra measured after 100 pulses and 2500 pulses when saturation has been achieved (Figure 3). This change is attributed to different growth and decay dynamics of the various intrinsic defect centers. The high laser-induced UV absorption still present after annealing at 400 °C suggests the formation of strong and very stable waveguides and gratings by UV laser exposure.

Tb^{3+} doping causes laser-induced absorption in both visible and UV spectral region (Figure 5). This is attributed to sensitizing effect on the formation of intrinsic hole and electron centers in contrast to the laser-induced photooxidation of Eu^{2+}, which suppresses the formation of intrinsic hole centers in the visible region[8].

Using fiber-launch set-up for projection of near-field images of waveguides on an image screen, very pronounced waveguides could be seen with the naked eye for the $FP_M/Eu^{2+}/0.3$ sample having higher Eu^{2+} concentration. In the less Eu^{2+} doped sample, $FP/Eu^{2+}/0.2$, and in the $FP/Ce^{3+}/1.0$ sample, less intense waveguides could be seen. Still lower intensities are observed for the Tb^{3+} doped UP glass (Figure 6). Only a few very weak waveguides are found for $FP/Ce^{3+}/0.5$ and $FP/Pb^{2+}/1.0$ samples. No significant waveguides could be detected in the undoped samples. This qualitative characterization of the laser-imprinted waveguides indicates that Eu^{2+} is a very effective dopant for creating photosensitive glasses followed by Ce^{3+} and Tb^{3+}. More pronounced waveguides are obtained at higher concentrations of the photosensitive Eu^{2+} and Ce^{3+} dopants.

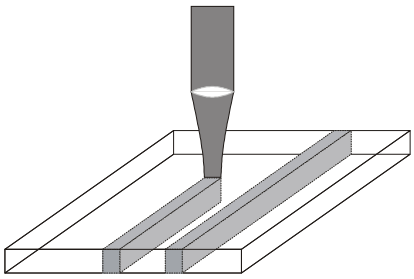

Figure 1: Sketch of experimental set-up for direct waveguide writing.

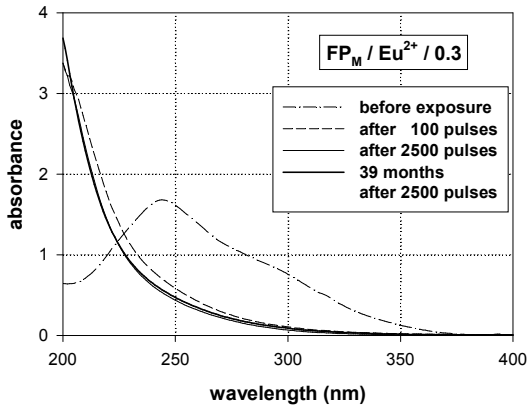

Figure 3: Absorption spectra of $FP_M/Eu^{2+}/0.3$ sample (2 mm thickness) before, immediately after and 39 months after laser exposure at 248 nm.

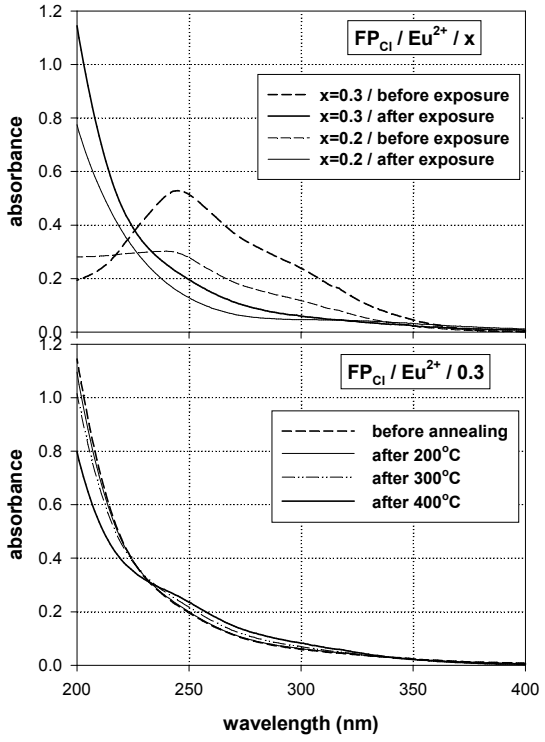

Figure 4: Absorption spectra of FP_{Cl}/Eu^{2+} samples (0.5 mm thickness) before and after laser exposure at 244 nm as well as before and after annealing of the laser-exposed sample at different temperatures.

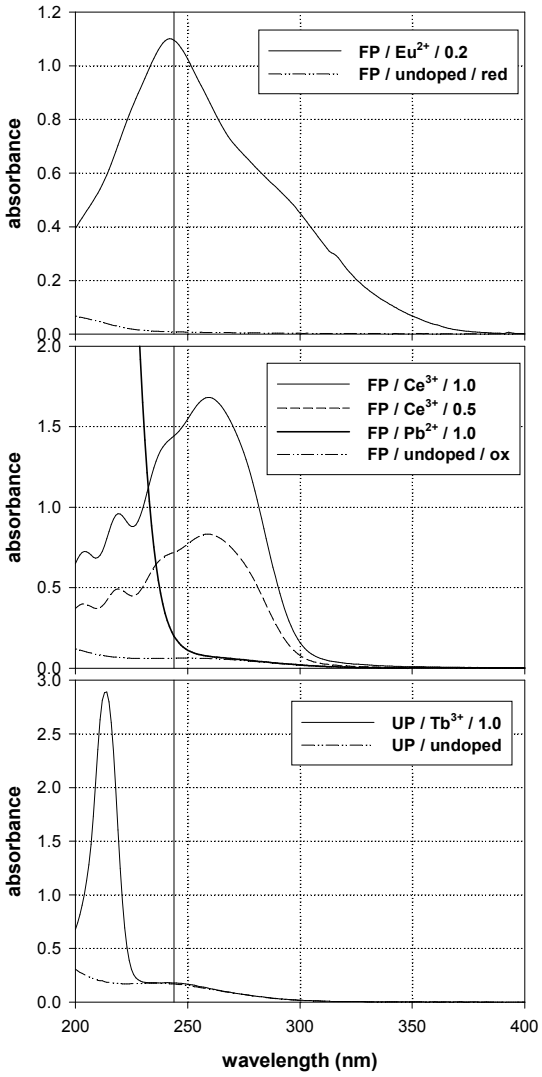

Figure 2: Absorption spectra of samples (2 mm thickness) before UV laser exposure. The laser wavelength of 244 nm is marked as thin line.

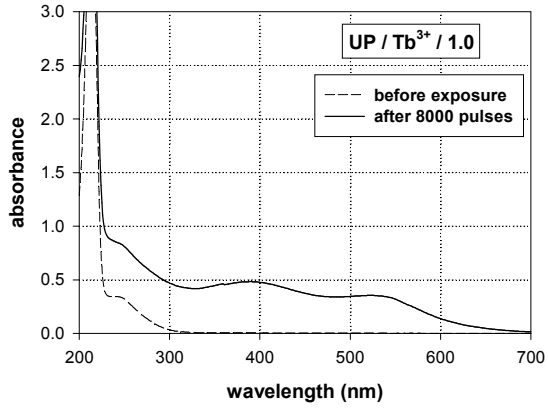

Figure 5: Absorption spectra of $UP/Tb^{3+}/1.0$ sample (4 mm thickness) before and after exposure at 248 nm.

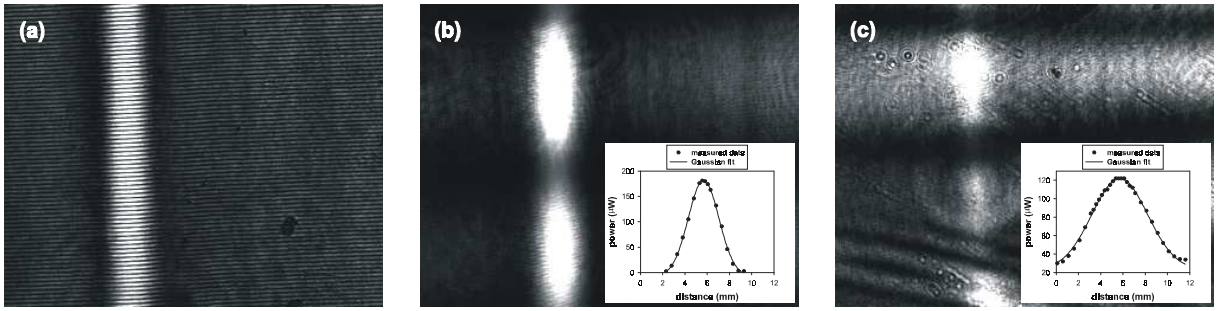

Figure 6: Near-field images of waveguides written in $FP_M/Eu^{2+}/0.3$ (a,b) and $UP/Tb^{3+}/1.0$ (c) samples using 150 mW laser power and 20 mm/min scan speed. Light was launched into the waveguides about 1 mm beneath (a) and very near to (b,c) the sample surface exposed to laser radiation. The exposure time of the CCD camera is 50 µs (a), 30 µs (b) and 100 µs (c). The insets show the mode profiles measured in the far-field by launching light very near to the exposed sample surface.

In the Ce^{3+} and Pb^{2+} doped FP samples as well as in the undoped and Tb^{3+} doped UP samples used for waveguide writing, photodarkening was observed in the form of brownish lines whose intensities decrease clearly from the laser exposed surface. The penetration depth of these lines visible with the naked eye correlates with the effective penetration depth of the laser beam calculated from absorption spectra (Table 2). In agreement with this result, clear waveguides are only observed close to the laser-exposed sample surface.

In both Eu^{2+} doped FP samples used for waveguide writing, strong light guiding is still observed 1 mm beneath the laser-exposed surface (Figure 6). This is in contradiction to the small effective laser penetration depth of 0.5 mm calculated from absorption spectra before laser exposure. However, this result agrees with the bleaching effect at the laser wavelength demonstrated by the laser-induced absorption spectra (Figure 3).

Using optical microscope and surface profilometer, no glass damage or changes of the sample surfaces have been observed, indicating the absence of volume changes due to laser exposure. Thus, the refractive index increase responsible for the waveguide creation in the samples is ascribed to laser-induced absorption increase according to the color center model[9].

---

[1] K. O. Hill and G. Meltz, J. Lightwave Technology 15, p. 1263 (1997).

[2] G. M. Williams, T.-E. Tsai and et al., J. Lightwave Technology 15, p. 1357 (1997).

[3] X.-C. Long and S. R. J. Brueck, Appl. Phys. Lett. 74, p. 2110 (1999).

[4] M. J. Weber, J. Non-Cryst. Solids 123, p. 208 (1990).

[5] H. Ebendorff-Heidepriem, D. Ehrt and et al., Proc. SPIE 3942, p. 29 (2000).

[6] H. Ebendorff-Heidepriem and D. Ehrt, Opt. Mater. 15, p. 7 (2000).

[7] D. Ehrt, M. Carl and et al., J. Non-Cryst. Solids 177, p. 405 (1994).

[8] H. Ebendorff-Heidepriem and D. Ehrt, Phys. Chem. Glasses. (In publication)

[9] A. Othonos, Rev. Sci. Instrum. 68, p. 4309 (1997).